UNCLASSIFIED

AD 273 655

Reproduced
by the

ARMED SERVICES TECHNICAL INFORMATION AGENCY
ARLINGTON HALL STATION
ARLINGTON 12, VIRGINIA

UNCLASSIFIED

NOTICE: When government or other drawings, specifications or other data are used for any purpose other than in connection with a definitely related government procurement operation, the U. S. Government thereby incurs no responsibility, nor any obligation whatsoever; and the fact that the Government may have formulated, furnished, or in any way supplied the said drawings, specifications, or other data is not to be regarded by implication or otherwise as in any manner licensing the holder or any other person or corporation, or conveying any rights or permission to manufacture, use or sell any patented invention that may in any way be related thereto.

ASTIA 273655
CATALOGUED BY ASTIA AS AD NO.
NOX

AFOSR 2294

AN ELECTROMAGNETIC SUSPENSION SYSTEM FOR THE MEASUREMENT OF AERODYNAMIC CHARACTERISTICS

Prepared by: H. M. Parker
J. E. May
G. S. Nurre

Contract No.: AF 49(638)-1022

Project No.: 9783

Task No.: 37725

ASTIA
RECEIVED
APR 2 1962
62-2-6
TISIA B

Research Laboratories for the Engineering Sciences

University of Virginia

Charlottesville

Report No. AST-4443-106-62U

March 1962

AN ELECTROMAGNETIC SUSPENSION SYSTEM FOR THE MEASUREMENT OF AERODYNAMIC CHARACTERISTICS

Prepared by: H. M. Parker
J. E. May
G. S. Nurre

Approved by: 

John E. Scott, Jr.
Acting Head, Astronautics Division

Contract No.: AF 49(638)-1022

Project No.: 9783

Task No.: 37725

RESEARCH LABORATORIES FOR THE ENGINEERING SCIENCES
UNIVERSITY OF VIRGINIA
CHARLOTTESVILLE, VIRGINIA

Report No. AST-4443-106-62U
March 1962

Copy No. 8

TABLE OF CONTENTS

LIST OF ILLUSTRATIONS

ABSTRACT

The design concepts are presented for a free electromagnetic suspension system functioning as force balance yielding simultaneous and independent measurements of force in three mutually perpendicular directions. The system is adapted to function as a wind tunnel balance which requires no physical attachment to the model under study. The concepts have been reduced to practice in a first-generation balance which is to be applied to the study of low-density sphere drags as a first demonstration of the unique capabilities of this balance system. The first model also is intended to serve as a test device to provide design information for a second-generation balance for the study of dynamic stability. The apparatus is described in detail and calibration procedures and future applications are discussed.

SECTION I
INTRODUCTION

During the past several years, a research program to study the feasibility of an electromagnetically supported gyroscope has been active in the Research Laboratories for the Engineering Sciences at the University of Virginia. During the course of this research, a 3-dimensional electromagnetic support was designed which provides for the simultaneous, and yet independent, measurement of the forces on a magnetic body in three mutually perpendicular directions [1]. The successful experimental demonstration of this device [2] marked an important step forward in the development of free electromagnetic suspension techniques which began at Virginia in 1937 [3], and has been summarized in detail in the literature by Beams [4]-[6]. The earlier devices supported actively in one dimension only and stability in the other directions depended upon fringing magnetic flux from the main field.

The use of the 1-dimensional electromagnetic support as a tool for the determination of small changes in weight or force had been clearly demonstrated by Beams [7] in 1950, but the application of these techniques to a wind tunnel balance did not seem practical unitl the theoretical work of Parker and Jenkins began to indicate that an isotropic 3-dimensional support system was a realistic possibility. The concept of the 3-dimensional electromagnetic wind tunnel balance was first presented by Kuhlthau [8] in 1957.

The present contract, which was started in January of 1961, is the first serious effort to reduce the concept to practice. The objective of the work is to construct a small balance system suitable for application to the study of sphere drag in low-density flows, and, in addition to making measurements of this type, to use the balance to develop design relationships to permit the construction of a second more versatile balance. A brief summary of the theory of the balance operation is given in Section II. However, many of the important quantities cannot be calculated exactly for all conditions of use and, hence, must be obtained experimentally.

The ultimate objective of the program is to apply the second-generation balance to a study of the dynamic stability of simple shapes supported freely (magnetically) at their center of gravity. It is hoped that measurements can be made in both continuum and free molecule regimes, as well as in the intermediate regimes.

This document has no particular milestone to report. The first model of the balance has been built and calibration is now in progress. The measurement program will continue under the support of an AFOSR grant which replaces this contract. Thus, this report will be concerned primarily with a discussion of the principles underlying the balance design and a description of the first model.

SECTION II
ELECTROMAGNETIC SUSPENSION TECHNIQUES

Basically, free support systems can be discussed from a unified point of view. There must be a field in existence, and there must be some property in the object to be supported which responds to the field to produce a force. Either electromagnetic or electrostatic fields are possible, but experience at the University of Virginia has indicated that high force-to-weight ratios are most readily obtained with electromagnetic systems. Hence, the discussion shall be confined to this family of systems, although for the most part, it is perfectly applicable to both families.

Next, support types can be divided into two classes: inherently stable and inherently unstable. The inherently stable supports are, of course, the simplest in principle, and most desirable. Unfortunately, they are also the most difficult to attain. Earnshaw's well-known theorem of electrostatics, which imposes severe restrictions on stable supports, states essentially that support of a body of fixed charge distribution by fixed fields cannot be stable in all directions; i.e., there is at least one direction in which the supported object will tend to move out of the field if displaced infinitesimally from the null position. Therefore, in effect, this null position cannot be used. Because of the similarity of electrostatic and magnetostatic field theory, it is found generally that this theorem applies also to magnetostatics.

Thus, to have a stable support, there must be at least one field component which can be varied to provide a force balance on the supported object. To date, there has been only one field proposed and demonstrated which is capable of meeting this condition inherently; i.e., in inherently stable support. This field relies upon the properties of superconducting materials (see, for example, [9],[10]). However, if the support is to be useful to measure forces or changes in forces, some method of readout is required and this is extremely difficult to provide in the case of this superconducting phenomenon. Therefore, at least at the present time, one is required to consider unstable supporting systems. Fortunately, stability is relatively easy to provide and the readout system for the forces is also straightforward.

In an inherently unstable support, stability usually is achieved by the use of a servo system which varies the field in the manner appropriate to effect the force balance. Let us consider then the elements of a servo system. The following components are required:

1) A device for controlling some property of the field, say its magnitude or its gradient, which will alter the interaction force on the body to be supported, and, hence, adjust the force to bring the force balance equation to equilibrium at least momentarily. In the simplest terms, the relationship between force and properties is

$$\vec{F}_I = (\vec{M} \cdot \nabla) \vec{B} \qquad (1)$$

where

$\vec{F}_I$ = body-field interaction force

$\vec{M}$ = magnetization vector in body

$\nabla\vec{B}$ = gradient of the magnetic field.

In the case of the wind tunnel balance, F_I must equal the aerodynamic force in a given direction, plus whatever tare forces, such as body weight for example, exist in that direction. It turns out that the maximum values of force/weight can be balanced when the maximum possible magnetic moment is generated in the body and the force is controlled by controlling the gradient of the field. Measurement of the force is accomplished by monitoring the current necessary to effect the changes of field gradient required by the force changes.

2) In order to activate the control field, some property of the body relative to the interaction force must be sensed. Customarily, this is the position of the body in the field. Such a device must be sufficiently sensitive to provide the information required by the servo system quickly enough to prevent the disturbing forces

from building up beyond control. It must provide unique information and, to maintain this uniqueness, it must be insensitivie to stray effects. The sensing device itself is often dependent upon the size, shape, and composition of the supported body. The development of a proper sensing device for the dynamic stability measurements is foreseen to be one of the major instrumentation problems of this program.

3) A mechanism must be provided to close the loop between the detection of the deviation of the system from its equilibrium state by the sensing element, and the change in the field interaction force which will restore the system to equilibrium. Here one is concerned with what might be called the "tightness of the loop." This ultimately will determine the total force/weight ratio which can be accommodated in the balance. The response time of the sensor is a premium factor. Finally, the "error" signal received from the sensor must be mixed with the proper "error derivative" signals to prevent the establishment of an oscillatory system of such magnitude as would limit its usefulness.

The reduction to practice of the above principles can be done in many ways. Since in a wind tunnel balance, as high a value of force/weight as is possible will almost always be desirable, the following discussions are restricted to the case of maintaining a saturation magnetization vector in the supported object. At least two methods of operation have been demonstrated to be feasible through many applications over the past several years.

Type I

Both $\vec{M}$ and $d\vec{B}/dz$ are controlled by the same set of coils. (The z direction is assumed to be the direction of desired support control.)

A multiplicity of supporting coils are used with coils located both above and below the supported object. If these coils are placed in a symmetrical fashion with respect to a horizontal plane through the point of support, it can be shown simply by adding up fields due to all the solenoids, that the field intensity $\vec{B}$ and all the even derivatives of $\vec{B}$ are proportional to the sum of the currents in the coils, and all odd derivatives of $\vec{B}$ are proportional to the difference of these currents.

Considering, for example, two coils, one above and one below the point of support, the following relations exist:

$$\vec{B} = k_0 (J_1 + J_2)$$

$$\vec{B}' = \frac{d\vec{B}}{dz} = k_1 (J_1 - J_2)$$

$$\vec{B}'' = \frac{d^2\vec{B}}{dz^2} = k_2 (J_1 + J_2) \text{ etc.,}$$

where the J's are the current densities in the respective coils and the k's depend upon the geometry involved. Such a system was experimentally demonstrated by Davisson and Beams [11] in 1953.

Type II

$\vec{M}$ and $d\vec{B}/dz$ controlled by separate coils. In this approach, a fixed current can be used in a single coil to generate a saturating field to provide the large magnetic moment. An independent set of small coils then can be used, one above and one below the supported object to alter the gradient of the field about the point of support. The 3-dimensional support system as first reduced to practice by Fosque and Miller [2] was of this type.

Before discussing these systems further, it is imperative to note an important point about sensing systems. By far the simplest sensor is a few turns of wire located somewhere near the supported object. This small coil is made an integral part of a tuned circuit in the servo loop, and the motion

of the support object toward or away from the coil affects the tuning of the circuit and, hence, generates the "error" signal. Such a detector is not very practical for use in the wind tunnel balance concept for two reasons. First, it becomes insensitive unless located very close to the magnetic material. This may be impossible in the case of a plastic model with only a small piece of magnetic material at its center. (The magnetic material must have spherical symmetry to eliminate magnetic torques on the body as it changes position in a 3-dimensional system.) In any event, it is not desirable to mount the coil inside the wind tunnel, as this would certainly introduce an unnecessary flow disturbance. Second, when the magnetic object to be supported becomes saturated, its permeability approaches that of free space and its effect on the coil is minimized. Consequently, some other sensor is required for the wind tunnel balance. An optical method is the one usually chosen.

A schematic of a typical Type I operation with an optical sensor is shown in Figure 1. A light source is mounted in an enclosure, and its rays are collimated into a beam which is partially interrupted by the supported sphere. The transmitted light is then focused on a phototube. Any change in the position of the sphere changes the amount of light falling on the phototube, which, in turn, produces an "error" signal. Since it is apparent that any minute fluctuation in the intensity of the light source will contribute also to this error signal, this effect must be eliminated from consideration. This is usually done by allowing light from the source to fall uninterrupted on a second photocell, and thus, the difference signal from the two photocells will give a true error signal. This signal is therefore the input to an appropriate electronic assembly which mixes with it the proper derivatives and uses the result to control a power amplifier to make the necessary corrections to the field coil currents. Usually, one field coil operates at fixed current, and the other is controlled by the servoed power supply, although the control can be applied to both coils if desired.

A typical Type II schematic is shown in Figure 2. The primary difference is that the currents to be servoed are now relatively quite small compared to those in Type I. The saturating field can be supplied by an

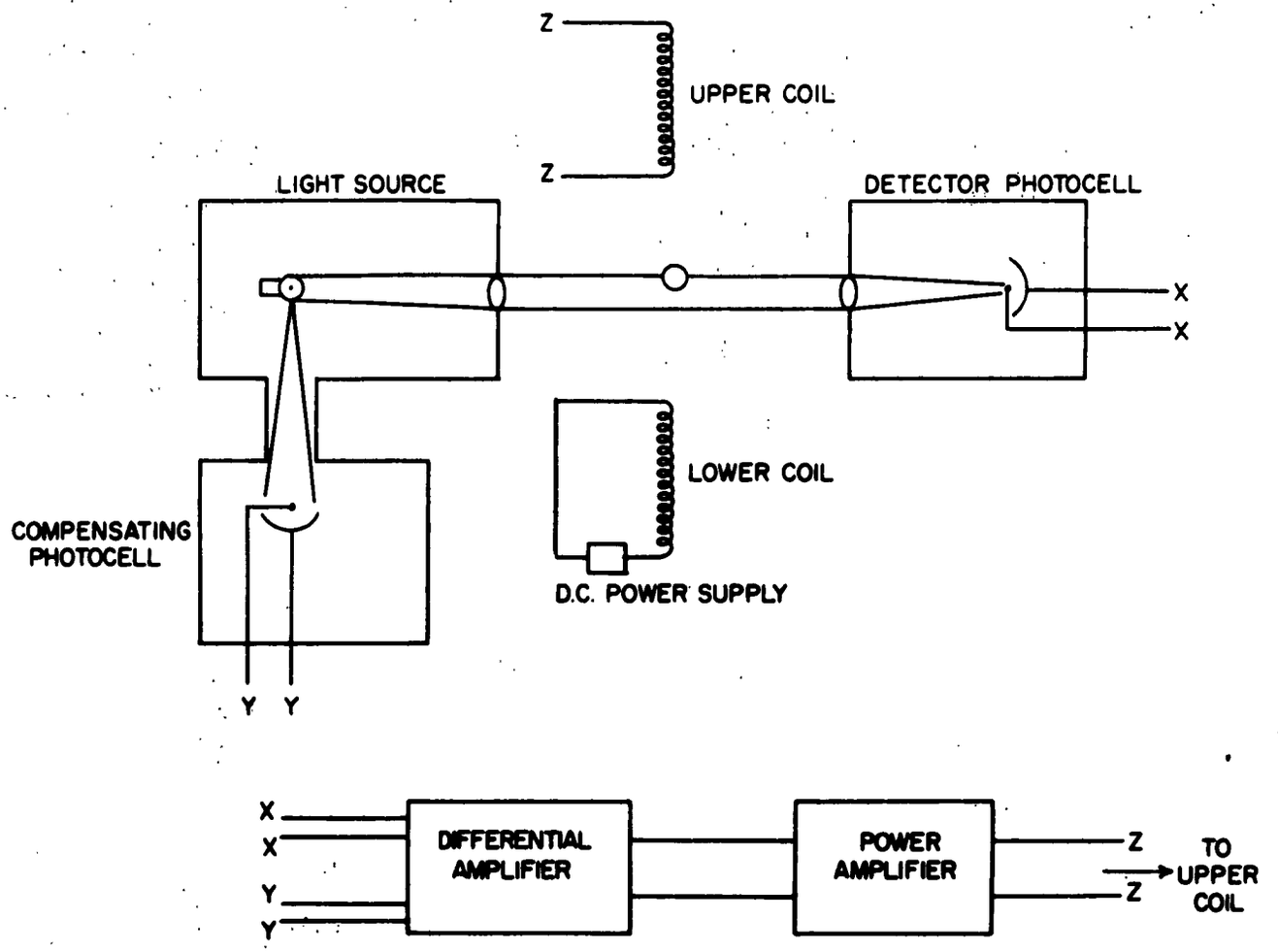

FIGURE I

SCHEMATIC OF
TYPE A GRADIENT CONTROL SYSTEM

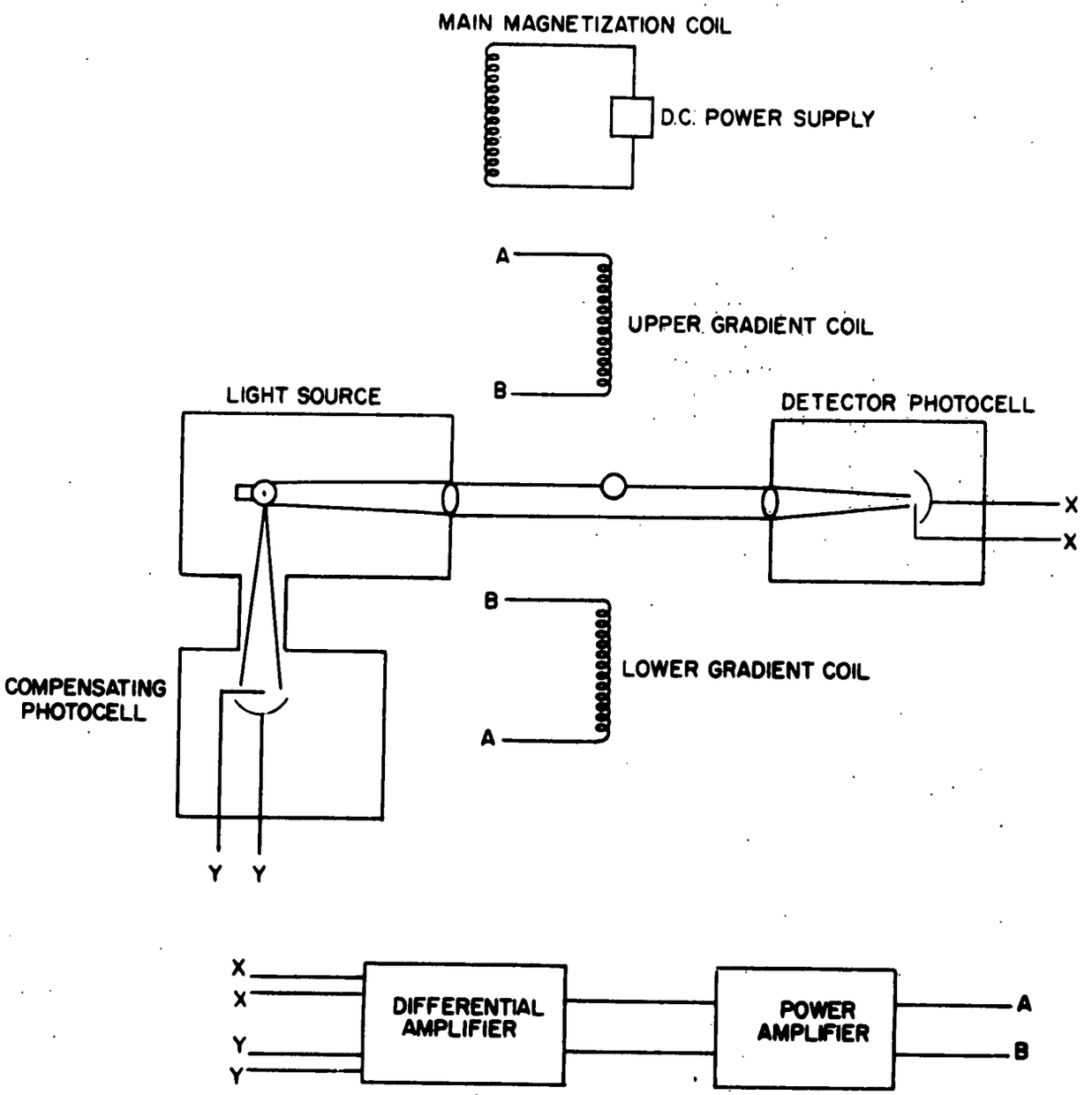

FIGURE 2
SCHEMATIC OF TYPE B GRADIENT CONTROL SYSTEM

iron core magnet using a fixed current. The gradient coils are usually arranged one above and one below the supported object, and, if the pair is connected in series opposition, a field is produced which has zero intensity midway between the pair and, thus, is small anywhere within a reasonably small object. Nevertheless, $d\vec{B}/dz$ will have large values over the magnetic sphere, and a wide range of support forces can be accommodated. The ampere-turn requirements are not large in the gradient coils even for the accommodation of a considerable range of forces.

There are many variations of electronic circuits which can be used in connection with either type operation. Usually, they are tailored to meet the specific end need. The particular circuits for the UVA-balance are discussed in the next section, and no particular value is to be obtained from any general description at this time. Although the basic principles presented thus far are quite general, the particular illustrations used have been restricted to supporting against force fields in one dimension only. The contribution of Parker [1] was a thorough theoretical study of the possibility of extending the basic principles to achieve independently controllable support in three mutually perpendicular directions.

Equation (1) (see page 4 of this report) is the starting point for the theoretical development of the isotropic EM support system, which is based upon the following two assumptions:

1) The body to be supported has a constant spherically symmetrical distribution of dipole moment per unit volume, $\vec{M}$. Normally, the magnetic part of the support body is considered to be a sphere with its state of magnetization either a) induced by a large constant magnetizing field or b) a result of being permanently magnetized and having its orientation fixed; e. g., by some external magnetic field.

2) The gradient field which is to produce the force on the sphere is axially symmetrical about a line through the center of the sphere.

If the main, magnetizing or orientating, field is uniform, it will not contribute a force on the sphere, and the $\vec{B}$ in equation (1) may be taken as the gradient field(s) alone. Consider the following system:

x_0, y_0, z_0 -- fixed reference system;

$\vec{M}$ -- constant magnetization vector, parallel to the z_0 axis, of a sphere whose center is at the origin;

$\vec{B}$ -- a (gradient) field whose axis of axial symmetry lies in the x_0z_0 plane and passes through the origin;

α -- the angle between the z_0 axis and the gradient field symmetry axis (see Figure 3);

β -- the angle between the resultant force on the sphere (also in the x_0z_0 plane) and the z_0 axis (see Figure 3).

A straightforward evaluation of equation (1) for this system leads to the result

$$F_{x_0} = 3\pi MC \sin\alpha \cos\alpha$$

$$F_{y_0} = 0$$

$$F_{z_0} = \pi MC (2\cos^2\alpha - \sin^2\alpha)$$

where

$$C = \int_{\text{sphere}} \frac{\partial B_z}{\partial z} \rho d\rho dz \quad ,$$

and in the expression for C, z and ρ are cylindrical coordinates for a coordinate system whose z axis coincides with the symmetry axis of the gradient field and whose origin is also at the center of the sphere. The direction of the resultant force is given by

$$\tan\beta = 3\tan\alpha/(2 - \tan^2\alpha)$$

and the magnitude by

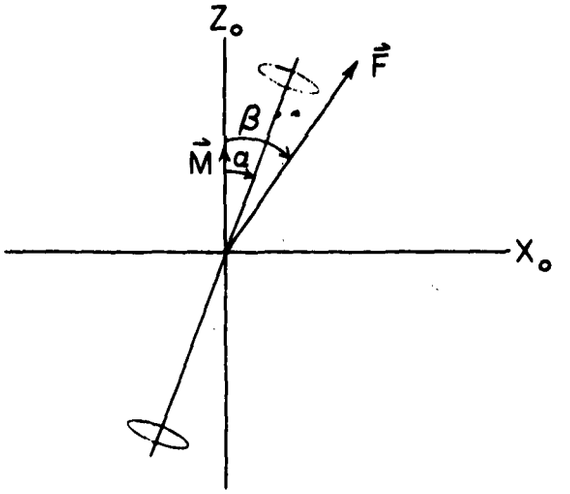

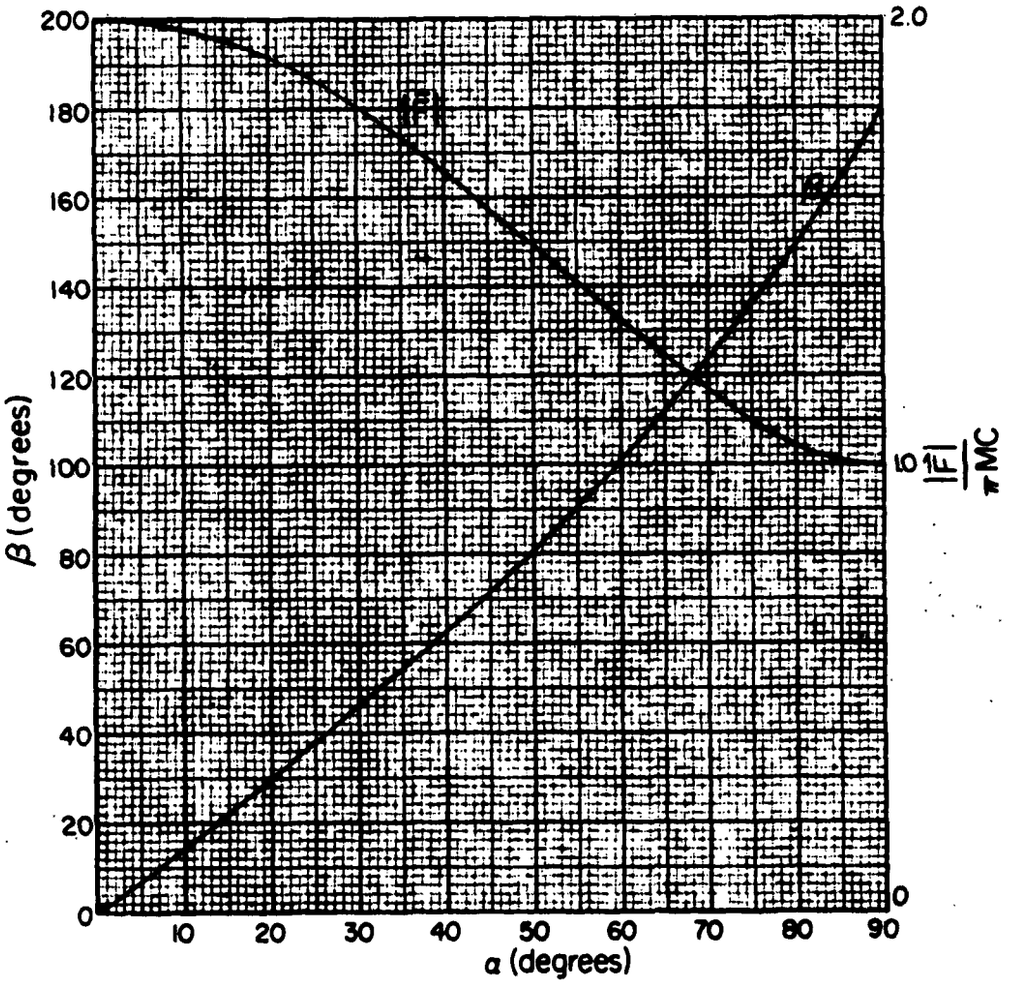

FIGURE 3

DIRECTION AND MAGNITUDE OF FORCE
DUE TO ONE GRADIENT COIL SET

$$|\vec{F}| = \pi \vec{M} C \sqrt{1 + 3\cos^2 \alpha} \quad .$$

Graphs of β and $|\vec{F}|$ are shown in Figure 3. For a given sphere and magnetization vector, the magnitude and sign of the force is varied by varying the magnitude and sign of the gradient field.

The problem of the 3-dimensional support reduces to that of finding the appropriate orientations of three gradient fields such that the three resultant forces are mutually perpendicular. A first interesting result is that if the three gradient field axes are mutually perpendicular, the resultant force is, in general, confined to a plane whose orientation depends upon the orientation of $\vec{M}$ with respect to the gradient field axis. In the special case that $\vec{M}$ is parallel to one of the perpendicular axes, the resultant force is always parallel to $\vec{M}$, a result which follows from the fact that $\beta = 0$ for $\alpha = 0$ and $\beta = \pi$ for $\alpha = \pi/2$.

The general result is easily seen in the following manner. Let x, y, z be a coordinate system such that the three mutually perpendicular gradient field axes are coincident with the x, y, and z axes. We have seen above that if $\vec{M}$ is parallel to one, say the x axis, the resultant force is also parallel to the x axis. Suppose $\vec{M}$ lies in one of the coordinate planes, say the xy plane. The x and y gradient fields produce a force lying in the xy plane since for each, the force is in the plane determined by $\vec{M}$ and the symmetry axis. The z field also produces a force in the xy plane since $\beta = \pi$ for $\alpha = \pi/2$. In the general case, when $\vec{M}$ has nonzero x, y, and z components, the linearity of the problem and the results above enable one to write

$$F_x = (2k_x - k_y - k_z) M_x$$
$$F_y = (-k_x + 2k_y - k_z) M_y$$
$$F_z = (-k_x - k_y + 2k_z) M_z$$

where k_x, k_y, and k_z are variables depending upon the sphere and the gradient fields. Consider the vector A whose x, y, and z components are $1/M_x$, $1/M_y$, and $1/M_z$, respectively. Then

$$\vec{A} \cdot \vec{F} \equiv 0 \quad ,$$

showing that the resultant force $\vec{F}$ is confined to a plane perpendicular to a vector ($\vec{A}$) whose direction cosines are, respectively, inversely proportional to the direction cosines of $\vec{M}$.

The general problem of finding 3-dimensional configurations is a two-parameter problem which presumably has a double infinity of solutions and which may be seen in the following way. Consider the nine direction cosines of the three gradient field axes

$$\alpha_1, \beta_1, \gamma_1, \alpha_2, \beta_2, \gamma_2, \alpha_3, \beta_3, \gamma_3$$

which must satisfy the three conditions

$$\alpha_i^2 + \beta_i^2 + \gamma_i^2 = 1 \qquad i = 1, 2, 3 \quad .$$

Three orthogonality conditions are to be satisfied

$$F_i \cdot F_j = 0 \qquad i, j = 1, 2; 1, 3; 2, 3 \quad .$$

Finally, there is a one-fold degeneracy with respect to angular position about $\vec{M}$, which can be removed by requiring, for example, that one of the gradient axes is confined to a plane containing $\vec{M}$. Thus, the nine variables must satisfy seven conditions leaving two degrees of arbitrariness. The problem has been so defined [1], and some numerical investigations of its solutions have been made, however, with rather uninteresting results. The following two arrangements were found prior to this general formulation and remain the two most interesting arrangements.

A. $\tan^{-1}\sqrt{2}$ Configuration

Gradient field axis 1: Parallel to $\vec{M}$, force parallel to $\vec{M}$.
Gradient field axis 2: At angle $\tan^{-1}\sqrt{2}$ to $\vec{M}$, force $\perp \vec{M}$, in plane of 2 and $\vec{M}$.

Gradient field axis 3: Same as 2, but rotated 90°about M.

This is the original 3-dimensional configuration, and the one which has been experimentally verified [2].

B. Symmetrical Configuration

Gradient field axis 1: At angle $\tan^{-1}\sqrt{8}$ to $\vec{M}$, force in plane of 1and $\vec{M}$,at angle $\tan^{-1}\sqrt{2}$ with $\vec{M}$.

Gradient field axis 2: Same as 1, rotated 120° about $\vec{M}$.

Gradient field axis 3: Same as 1, rotated another 120° about $\vec{M}$.

Unit vectors along the force directions form a cube such that $\vec{M}$ is parallel to the main diagonal.

From the point of view that each gradient field is to be produced by two identical, coaxial coils symmetrically placed on either side of the sphere, the physical space available to place the coils is of primary importance. In the case of the wind tunnel, the necessity of providing space for the tunnel in which the supported body is to reside is of primary importance. For a given pair of gradient coils, the field gradient at a point on the axis midway between the coils decreases rapidly as the distance between the coils increases. On the other hand, at larger separations, there is room for larger coils with, consequently, more copper and power. Detailed considerations of this sort have indicated that the symmetrical configuration is the most suitable wind tunnel arrangement.

SECTION III
DESIGN CONSIDERATIONS FOR THE FIRST WIND TUNNEL BALANCE

The philosophy governing the design of the first balance includes the following points:

1) The first-generation balance should demonstrate the fundamental feasibility of the method;

2) It should enable the measurement of some interesting aerodynamic quantities, with existing or easily obtainable equipment;

3) It should enable, with as minor as possible modifications, the experimental investigations of problems and improvements expected in later generation balances;

4) The major goal of the EM balance development is the study of the dynamic stability of at least simple, aerodynamic shapes.

A careful consideration of these over-all objectives led to the present balance, which has the following important characteristics:

1) Fits around a nominal 3"-diameter circular test section;

2) Has nonmagnetic cores in main and gradient coils;

3) Sphere magnetization is induced by main field;

4) Supported body to be the bare sphere and sphere drag measurements to be made.

The basic problem of support is that of providing for a sufficiently large value of the product of the magnitude of the dipole moment per unit volume, $|\vec{M}|$, of the sphere and the gradient $\partial \vec{B}_z/\partial z$, of the gradient field. Concerning the first factor, if the problem were simply to support a sphere, it would be better to use a good permanent magnet material for the sphere, magnetize it permanently, and use a main field just large enough to keep $\vec{M}$ aligned sufficiently close to the tunnel axis. This follows from the general

fact that large magnetic fields are difficult and expensive to produce. However, such a permanently magnetized sphere, experiencing large torques tending to keep $\vec{M}$ aligned with the main field, would not be rotationally free as is desirable for dynamic stability studies. For rotational freedom, it is desirable to have the magnetization induced by the main field and, further, to have the rotational hysteresis and anistropy of the sphere as small as possible. Unfortunately, magnetic materials with low rotational hysteresis generally have low values of saturation magnetization. While spheres of any magnetic material may be used in the early phases of the program, the design was intended to enable the support of ferrites which have low rotational hysteresis. In the approximation that $\partial B_z/\partial z$ for a gradient coil is constant over the volume of the sphere, support capacity is independent of sphere size.

It must be noted that in the wind tunnel balance, additional forces in the direction of the tunnel axis may be obtained by deliberately unbalancing the currents in the main field coils to produce a gradient in the main field at the sphere. Thus, especially in a vertical wind tunnel where the weight of the support body and the aerodynamic drag are parallel, considerable force capacity in addition to that provided by the gradient fields is available. Even though the provision of such gradients in the main field tends to reduce the main field strength available, and, hence, the magnetization of the sphere, it is estimated that axial forces of the order of 10-50 g's are available by this method.

The problem of production of the main and gradient fields and how the problem scales with tunnel size may be appreciated by considering single turns of coils. First, consider the main field, and let us imagine building the two main field coils by adding two turns at a time, one to each main coil. The field produced at the center of the sphere by two symmetrically placed turns, each of radius a and axial distance b from the center of the sphere is

$$\vec{B} = \frac{4\pi I a^2}{(a^2 + b^2)^{3/2}} \qquad (2)$$

where I is the current in each turn. This may be rewritten as

$$\vec{B} = 4\pi I \frac{\sin^2 \theta}{r} \qquad (3)$$

where

$$r = \sqrt{a^2 + b^2} \quad \text{and} \quad \tan \theta = a/b \quad .$$

Thus, one can see that a/b should be as large as possible and that $\sqrt{a^2 + b^2}$ should be as small as possible. Contours of equal values of $\sin^2 \theta/r$ show the shape of the ideal coil. As the space available to build main coils is used, single turns contribute ever smaller amounts to the main field, while the power dissipation in a single turn, at constant I, increases as a. It is easy to see that liquid-cooled coils to increase current density become important in producing large fields.

To see how the main field problem scales with tunnel size, consider two tunnels with main coils of the same relative geometry, scaled by a linear factor f(f = 4 corresponds to going from a 3"-to-12"-diameter tunnel). Thus, areas increase by f^2 and volumes by f^3. The number of turns in the coil go as f^2, an area. From the expressions (2) or (3), one sees that the single turn expressions go as 1/f; thus, the total main field goes as $f^2(1/f) = f$. However, to pay for this, the power dissipation, which is proportional to the volume of copper, goes as f^3. If one wishes simply to produce the same field, the number of turns may be increased only as f, or somewhat less due to more efficient positioning of the turns, and the power dissipation goes as somewhat less than f^2. In any event, power dissipation is the most brutal fact of life with respect to nonmagnetic-cored main field coil design, especially as one goes to large tunnel sizes.

In looking forward to the design of a balance and tunnel system large enough to look promising for dynamic stability studies, it appears necessary to investigate the possibilities of using magnetic material circuits in the production of the main fields. The first balance is expected to be useful in this investigation.

Secondly, let us consider gradient field production in the symmetrical configuration. The relative position of the three gradient axes and the space occupied by the tunnel proper defines the space available to build gradient coils. It turns out that a gradient coil pair is confined to a double cone about the gradient field axis, vertex at the sphere center, of half angle $\tan^{-1} 1/\sqrt{2}$. Additionally, each cone is truncated by the tunnel cylinder. Again, a consideration of the contribution of symmetrical single turn pairs leads to a value of $\partial B_z/\partial z$ at the sphere center of

$$\left(\frac{\partial B_z}{\partial z}\right) = 12\pi I \frac{a^2 b}{(a^2 + b^2)^{5/2}} = 12\pi I \frac{\sin^2\theta \cos\theta}{r^2} \qquad (4)$$

where

I = current in each (opposing)

a = radius of each turn

b = distance of each turn from sphere center

$\tan\theta = a/b$

$r = \sqrt{a^2 + b^2}$.

Contours of $\sin^2\theta \cos\theta/r^2$ = constant give the shape of the ideal gradient coils. For constant r, equation (4) is a maximum at $\theta = \tan^{-1}\sqrt{2}$ while the maximum value of θ allowable in the symmetrical configuration is $\theta = \tan^{-1}(1/\sqrt{2})$. As the gradient coils are built by symmetrically adding pairs of turns, the contribution to $\partial B_z/\partial z$, for a given I, decreases as $1/r^2$. Obviously, turns at small θ (small a) are especially inefficient. However, since a numerical analysis indicated that coils of reasonable size, with current densities obtainable without cooling could provide gradients sufficient to support a ferrite sphere, liquid cooling and magnetic material cores were not designed into the first balance.

The scaling effect on field gradient production can be seen by assuming a linear scale factor f for two systems of the same relative geometry. The gradient goes as $1/f^2$ and the number of turns goes as f^2. Thus, the same

$\partial \vec{B}z/\partial z$ is produced. The volume of copper and the power dissipation goes as f^3. Even though the power dissipation in itself is not especially serious, control problems associated with voltage required and inductance become serious as the size increases. Therefore, in the design of the stability balance, the possibility of utilising liquid cooling and/or magnetic material cores must be considered seriously as a method of arriving at a more efficient balance. This follows from the rapid $(1/r^2)$ decrease of the contribution to $\partial \vec{B}z/\partial z$ of a turn pair with distance from the sphere. The first balance is expected to be useful in investigating the use of magnetic material cores for the gradient coil sets.

An essential factor in the operation of an EM balance is an arrangement to sense the position of the sphere and, thus, to provide the error signal link in the servo loop. The supported body for dynamic stability studies is envisioned as an aerodynamic model of nonmagnetic material with a magnetic material sphere embedded at or near its center of mass. The problem is to sense, continuously, the 3-dimensional position of the center of the sphere. Since physical sensors may not be placed inside the tunnel (except sufficiently far downstream of the model), the sensing system must operate from a considerable distance from the model. Since sensing methods based on inductive and/or capacitive effects become very insensitive at large distances, it has been assumed that optical methods would be most appropriate. For simple shapes of the supported body, appropriate systems of light beam have been very successful as position sensors.

For the initial phase with the first balance, spherical bodies are to be supported and the optical multiple beam method is quite satisfactory. However, when the model is considered to be, say, an ogive of revolution with tail fins, light beam detection of its center of mass, independent of its angular orientation over a suitable range, obviously becomes a more difficult problem. Position sensing is considered to be the major unsolved problem for the second-generation (dynamic stability) balance. It is expected that the first balance will be useful in finding a satisfactory solution to the position sensing problem.

It is perhaps pertinent to point out that when a reasonably complicated experimental arrangement is to be developed, it is often a more efficient process to gain experience initially with an inexpensive and simplified version, of course, embodying as many of the fundamentals as feasible. It is difficult to guess with adequate precision in the design stage all the actual physical problems which may arise in a novel arrangement. A case in point presently appears to be the problem of vibration in the first balance, which was given only casual consideration. The solution to this problem, an almost certain eventuality, will be a less expensive and time-consuming process in the first balance than it would have been in a balance four times as large.

SECTION IV
DESCRIPTION OF APPARATUS

The University of Virginia electromagnetic wind tunnel balance is of the "B" or symmetrical configuration type as described in Section III. Thus, it is quite different in concept from other electromagnetic balances described in the literature [12], [13].

The concept of the Virginia balance is shown schematically in Figure 4, and in model form in Figure 5. The size of the system is prescribed by establishing the diameter of the wind tunnel. After due consideration of the range of drag-to-weight ratio values to be encountered in continuum and low-density flow for various objects of interest; of the aerodynamic interference between model and cylindrical test section wall; of the practical limitation of accuracy of model construction versus model size; and, finally, of the capabilities of the air supplies available at Virginia, a diameter of 3-1/2 inches was chosen for the tunnel hole through the balance. This was based upon a drag/weight ratio of 3 as a probable value.

Referring to Figure 4, the magnetizing coils, A, are arranged in an axially symmetric manner about the tunnel centerline. These coils provide the constant saturation field at the model position. On the basis of the design studies for the first-generation balance, a magnetic moment of 0.1 webers/m^2 at the center of the sphere of magnetic material was established as the requirement. In order that a convenient coil size be obtained, a current density in the coils of 2×10^7 amps/m^2 was necessary and the conductor was chosen to be 1/8" copper tubing, through which cooling water was circulated. Teflon ribbon, one mil thick, was wrapped on the tubing to provide electrical insulation. Due to the small inside diameter of the tubing, and the associated pressure drop, it was found necessary to provide several parallel circuits for cooling water in each coil. The coils were wound on aluminum frames which can be seen at the top and bottom of Figure 6.

Three gradient coil sets, B, only one set of which is shown in Figure 4, are symmetrically placed in planes about the main field direction; i.e., about the tunnel centerline. The axes of these coil sets are oriented with

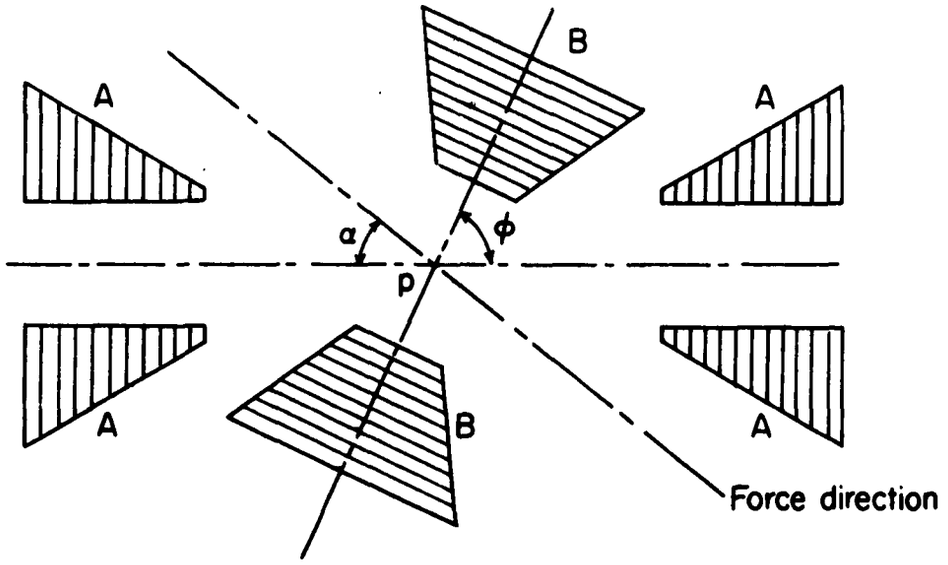

FIGURE 4

SCHEMATIC OF VIRGINIA
ELECTROMAGNETIC BALANCE CONFIGURATION

FIGURE 5

MODEL OF VIRGINIA ELCTROMAGNETIC BALANCE CONFIGURATION

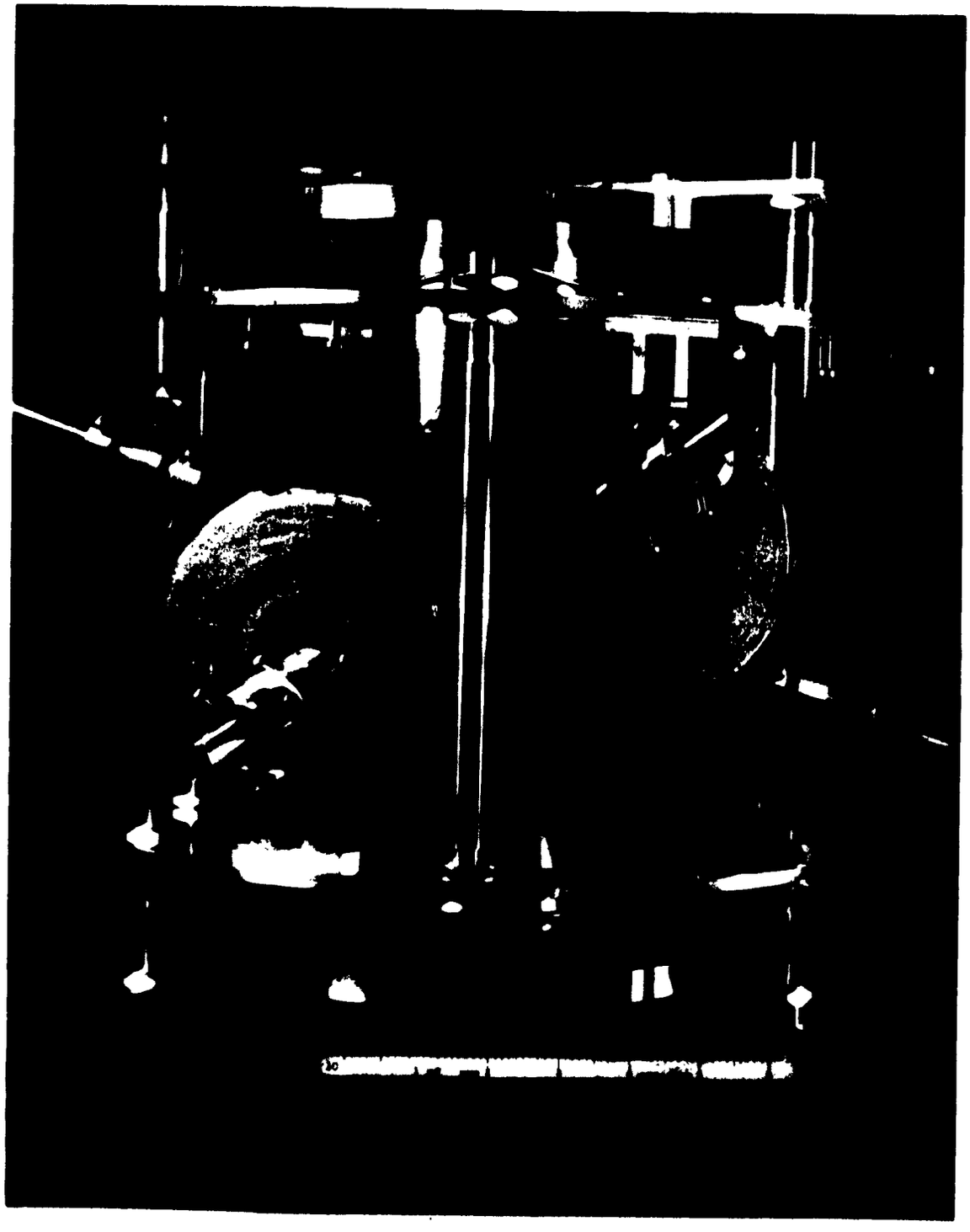

FIGURE 6
GRADIENT COIL SETS MOUNTED IN PLACE

respect to the centerline such that $\phi = \tan^{-1} 2\sqrt{2}$ (Section II). A current in a gradient coil set (equal and opposite currents in each coil of the pair) provides a force on the sphere in the plane defined by the gradient coil axis and the tunnel axis. This force makes an angle $\alpha = \tan^{-1} \sqrt{2}$ with the main magnetizing field as shown in Figure 4. With this orientation, the three gradient coil sets have force directions which are mutually perpendicular, lying along the edges of a cube, the body diagonal of which is the tunnel axis. The gradient coil sets are shown mounted in position in Figure 6. The tunnel axis is vertical in this picture as well as in Figure 7 which shows the entire balance assembled and ready for calibration. The gradient coils are wound with No. 26 wire conducting 0.5 ampere of current. Forced cooling is not necessary since the power dissipation is only 100 watts. As stated above, the gradient coil sets are inclined at particular angles relative to the balance centerline and to each other. Thus, in order to allow for alignment of the coils, each is attached to the balance frame by a support capable of allowing six degrees of freedom. They are wound on forms containing an axial aluminum tube through which a sighting may be made by telescope to assist in alignment. Crosshairs are placed on each end of the tube for this purpose.

The magnetic suspension system is inherently unstable, and a control loop is required. The position of the sphere is sensed by an optical system shown schematically in Figure 8, and this error signal is used to control the current in the gradient coils. Each of three light sources, one for each set of gradient coils, is collimated to provide a rectangular beam which is normal to the force direction of a gradient coil set with which it is associated. Each beam of light impinges on the sphere. The longest dimension of the beam of light is larger than the sphere diameter. For each light source, two photocells are positioned so that each cell is exposed to the light coming from a source and passing by the edge of the sphere. A movement of the sphere will cause a reduction of light in one cell of each pair and increase in the other, thus generating the control signal.

A block diagram of the control system is shown in Figure 9. Without the compensation block, the system is unstable and the sphere will not stay in support. A compensation network is required to provide this stability.

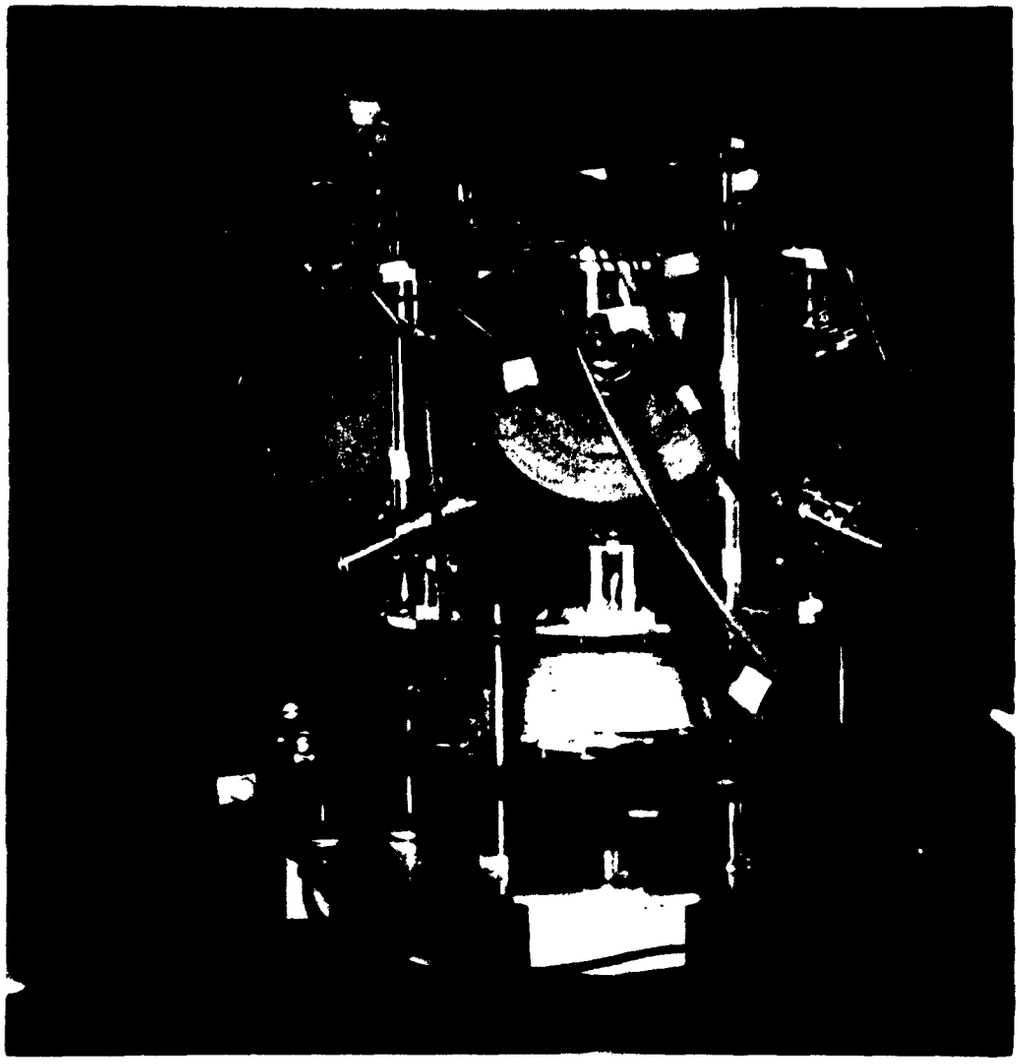

FIGURE 7
COMPLETE BALANCE ASSEMBLY

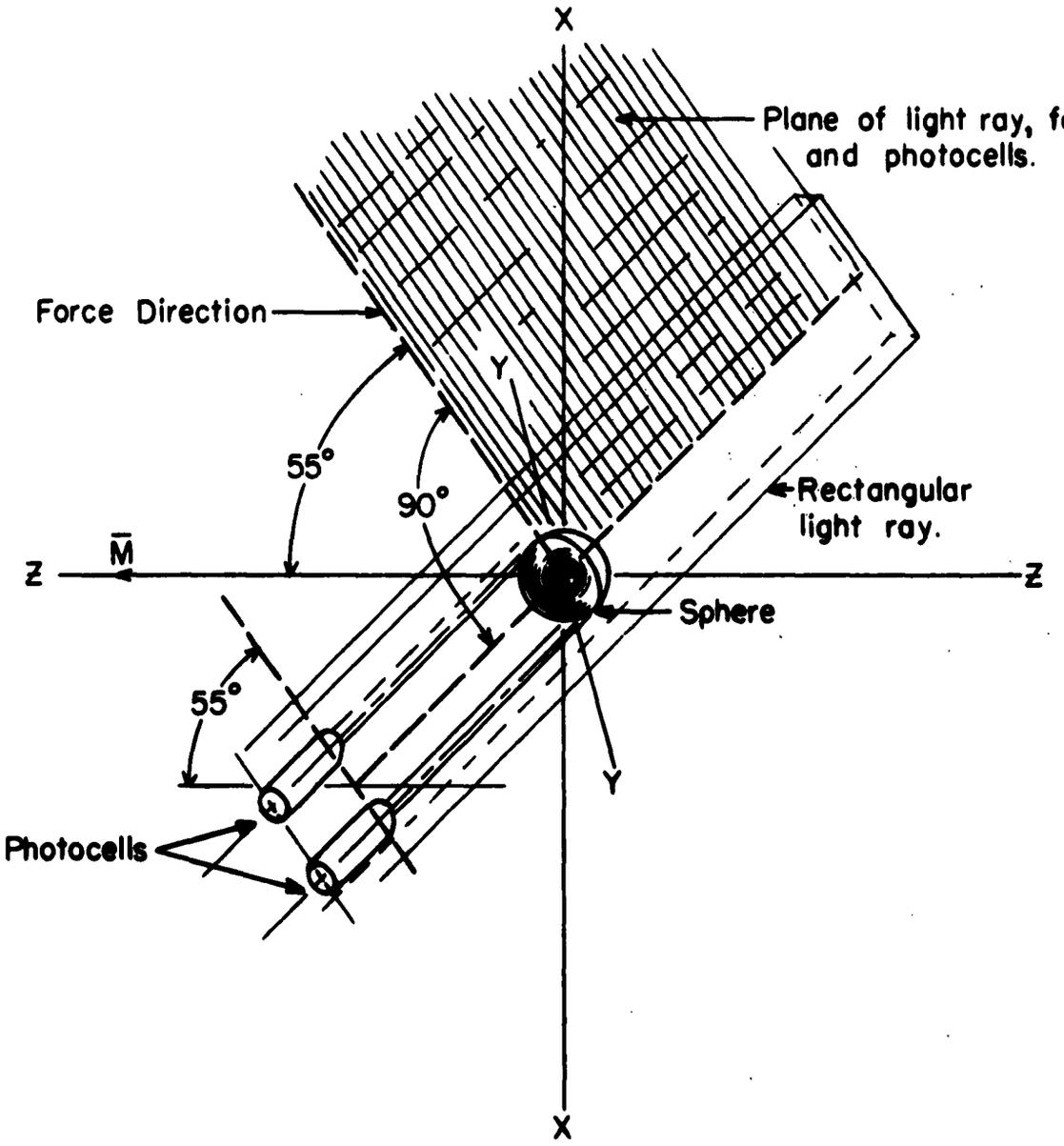

FIGURE 8

ORIENTATION OF OPTICS
RELATIVE TO ASSOCIATED FORCE DIRECTION

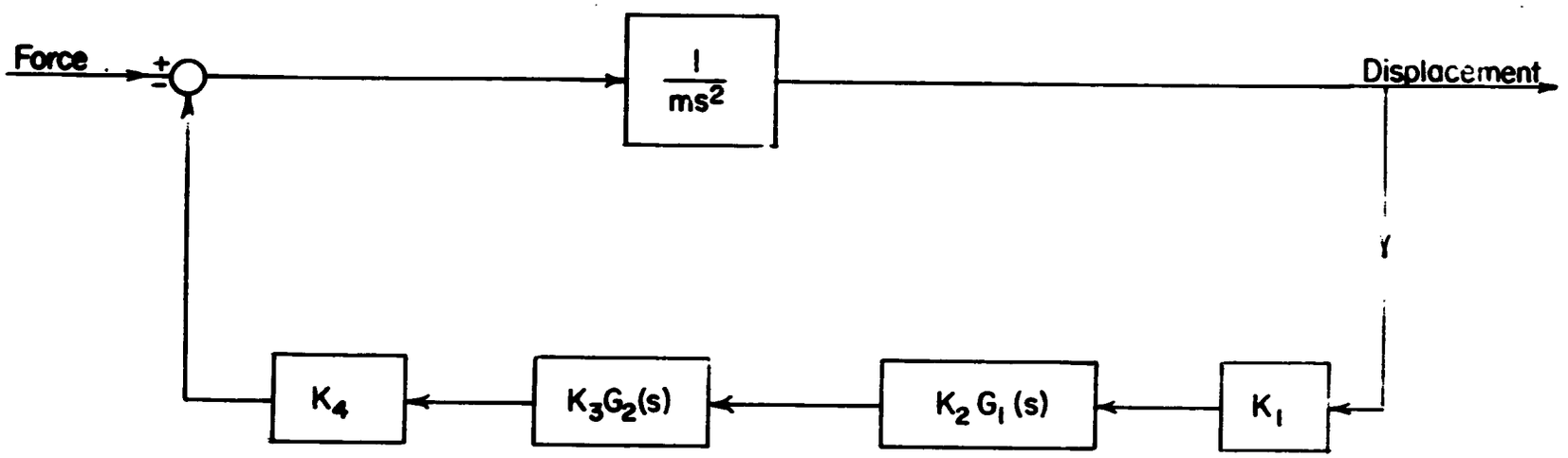

s - complex frequency
m - moss of sphere (kilogram)

K_4 - gradient coil gain

K_2 - gain of compensation network

K_3 - gain of driver for gradient coil $\left(\frac{amp}{volt}\right)$

K_1 - gain of photocell $\left(\frac{meters}{volt}\right)$

$G_1(s)$ - frequency dependent compensation network

$G_2(s)$ - frequency dependent part of driver stage

FIGURE 9

POSITION SENSING FEEDBACK SYSTEM

Typical electronic circuits are shown in Figures 10 and 11. Figure 10 shows the control circuit where the compensation network (in the dotted box) is followed by a variable gain amplifier. This circuit drives the power amplifier of Figure 11, this being designed to permit the current to be driven through the gradient coils in either direction.

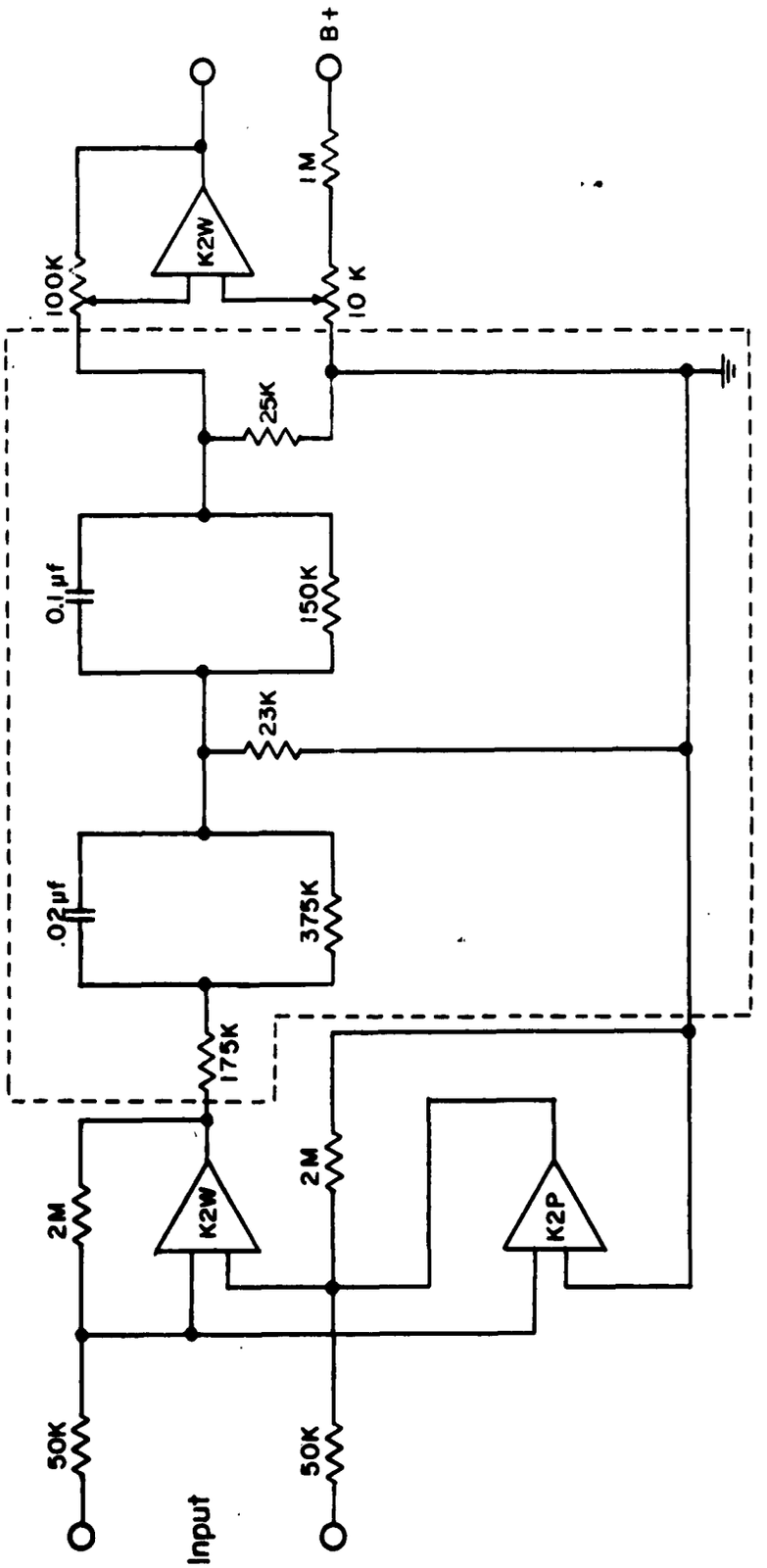

FIGURE 10

CONTROL CIRCUIT

4443-28

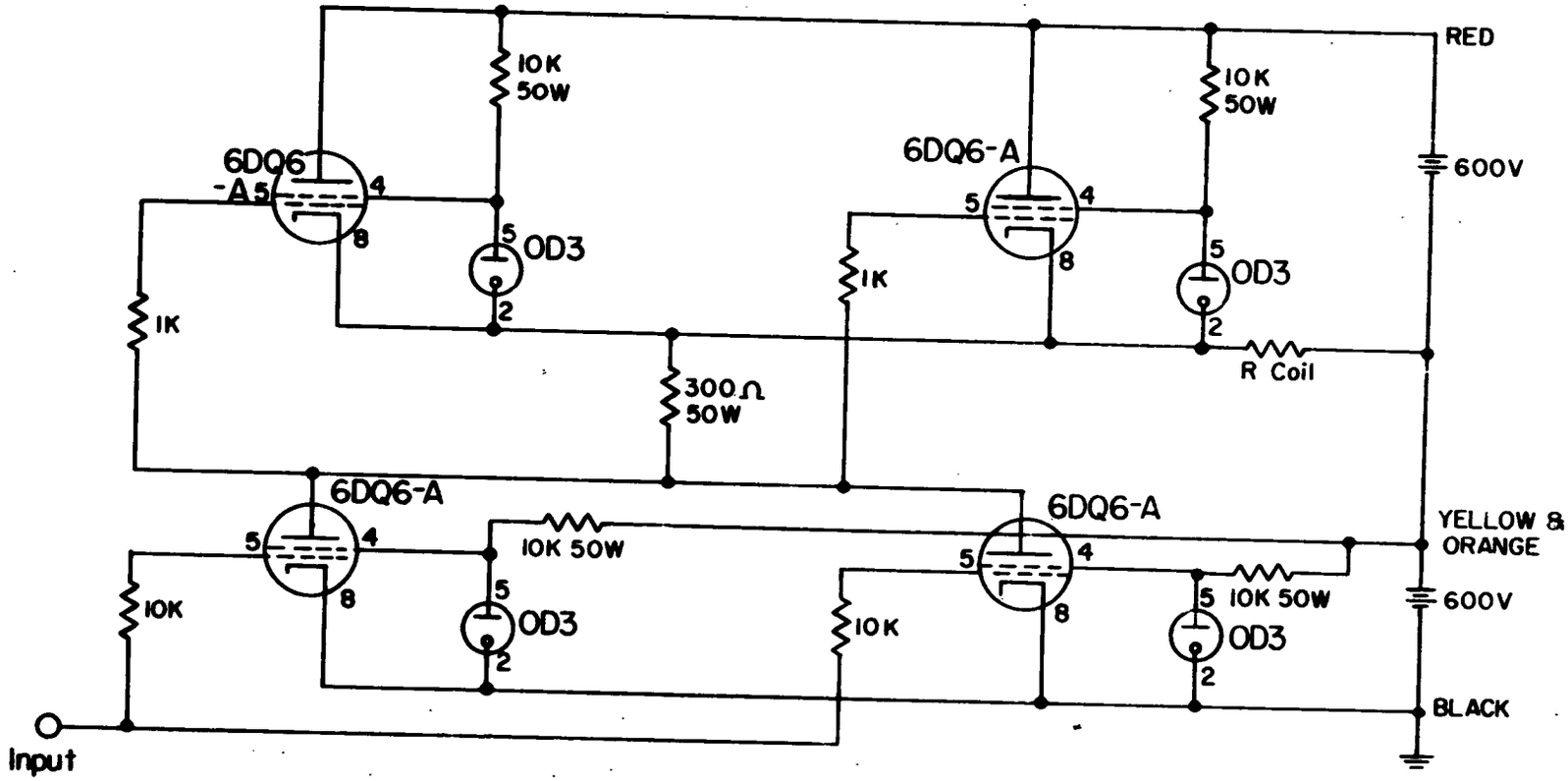

FIGURE 11

POWER AMPLIFIER

SECTION V
CALIBRATION OF BALANCE

One of the features of the EM balance is the fact that the forces exerted on the sphere to support the body stably are subject to measurement, in principle, with good precision. In dynamic stability studies, the net forces exerted on the model may or may not be of significant importance; if significant, they are available. In some applications; e.g., sphere drag (Section VI), the forces exerted on the supported body are important.

Originally, it was envisioned that the well-known sphere drag in low-speed continuum regime flow would be used to prove the balance and to calibrate it. This decision has been changed since continuum regime sphere drag, being well known, is basically uninteresting, and because simpler and quicker methods of proof and calibration of the balance are available.

Steady state calibration of the balance may be accomplished, and is presently so contemplated, by simply hanging weights on the supported sphere. Nonsteady state calibration and study of the balance may be effected, for example, by letting drops of a fluid fall on a pan hung from the sphere and/or letting drops of fluid fall from the pan. A combination of these methods should both prove and calibrate the balance. This process is being delayed at the moment because of some vibration difficulties which must be solved. The present state of calibration may be summarized as follows.

The main field coils were designed to produce, for a coil current of 190 amps, a field of 1000 gauss at the sphere position. For several reasons, including a decreased turn density (1/8"-diameter tubing was difficult to wind) and a larger than design distance between coils (liquid coolant connection required more space), the main field strength at the sphere, for coil currents of 165 amps, was 560 gauss. Especially since the bulk of the power required is associated with the main field production (about 20 kw for the first balance), it is felt that a more careful and better design of the main coils is very important in a larger balance.

The design field gradient, $\partial B_z/\partial z$, for one of the gradient coils sets was 26 gauss/cm at coil currents of 400 ma. The measured value of the gradient was 32 gauss/cm at the same current. The reason for the discrepancy is not definitely known.

Support of a ferrite sphere has been achieved, even though the vibration troubles have not yet been eliminated. A very rough calibration point has been made in the following manner. Two spheres of very nearly the same size but different magnetic properties and different densities were used. One was an ordinary ferrite and the other a ferrite with a considerable amount of plastic binder. The main field was unbalanced to provide part of the support. Assuming that the spheres were operating well below the knee of the magnetization curve (the main field was about 400 gauss), the magnetization can be calculated and the weights of the spheres measured. The two spheres were supported at different gradient coil currents. From the differences for the two spheres (weights and currents) and subtracting the main field contribution, the additional support force per unit gradient current was

0.0398 newtons/amp from sphere weights

0.0381 newtons/amp from directly-measured gradients.

Considering the uncertainities involved, the agreement is fortuitious. As soon as the vibration difficulties are eliminated or reduced sufficiently, a thorough calibration will be made.

SECTION VI
APPLICATION TO SPHERE DRAG

The drag of spheres in flow regimes between continuum and free molecule ($0.015 < Kn < 15$, where Kn is the Knudsen number) appears to be of special interest to the theorists who are attempting to develop the theory of rarefied gas dynamics. At the same time, it appears that experimental measurements of sphere drag in this range, so far, have been somewhat inadequate. Sphere drag measurements of good precision are especially suitable for even the first model of the EM wind tunnel balance.

As mentioned earlier, it was originally contemplated that the well-known sphere drag in the continuum regime would be used to prove and calibrate the EM balance. Having decided to calibrate by a simpler method, there still remains the objective of measuring sphere drag in the interesting rarefied range. The question of what part of this interesting range of sphere drag can be investigated, with the first balance and inexpensive, easily obtainable equipment, becomes of interest.

For a sphere, the Knudsen number is

$$Kn = \lambda/d_s$$

where λ is the mean free path in the flow and d_s is the diameter of the sphere. The mean free path is a function only of the density to a very good approximation and for air at room temperature may be written as

$$\lambda = 50/p$$

where λ is in mm and p is the static pressure in μHg. Irrespective of the Mach number of the flow, a Knudsen number range of

$$0.015 < Kn < 15$$

corresponds to

$$33 \times 10^2 > pd_s > 3.3 \quad .$$

Thus, the flow regime is fixed by the product of test section static pressure and sphere diameter to a very good approximation.

To make significant sphere drag measurements, there are two requirements which must be met, namely, the drag force must be of a magnitude such that it can be measured with suitable precision, and, secondly, the flow bathing the sphere must be known. The drag force is most suitably expressed as the ratio of drag to weight, since for spheres of a given material, the ratio of the force which the balance exerts on the sphere for fixed currents in all the coils to the weight of the sphere is essentially a constant. The drag-to-weight ratio, D/W, is

$$D/W = \frac{C_D(1/2\ \rho v^2)\ \pi/4\ d_s^2}{\frac{1}{6}\pi d_s^3\ \rho_s g} = \frac{3C_D}{2\rho_s g}\ (1/2\ \rho v^2)\ \frac{1}{d_s}$$

where ρ_s is the density of the sphere, g is the acceleration due to gravity, C_D is the drag coefficient, and $1/2\ \rho v^2$ is the dynamic pressure in the flow. For good measurements, D/W must not be so large as to exceed the force capacity of the balance and must be large enough so that the difference between total force and weight has sufficient accuracy. It is obvious that D/W may be adjusted over considerable ranges by varying $1/2\ \rho v^2$ and d_s. (With the simple tunnel systems to be used initially, it is expected that the stream velocities will be limited to values less than about 0.2 of the speed of sound.)

The problem of adequately determining the flow in the test section can be approached from two directions. First, the flow field may be surveyed with conventional pitot probes (continuum regime), going to pressures as low as are feasible. From considerations of probe-tunnel wall interference effects and continuum regime operation of the probe, it is estimated that the minimum pressure in the 3" tunnel is about 0.3 mmHg.

Estimating further that spheres as small as 1-mm diameter may be used, it is expected that Knudsen numbers less than and up to about 0.15 (roughly slip-transition boundary) may be investigated.

The second approach is that of using the free molecule probe, as developed by the Toronto group, to survey the flow. Here, from considerations of probe size and free-molecule regime probe operation, it is estimated that one can operate up to a maximum test section pressure of about 3 μHg. Assuming a maximum sphere diameter of 10 mm, it is estimated that Knudsen numbers of 1.5 and larger may be investigated.

Thus, with the first balance and the simple tunnels contemplated, it is likely that a portion of the interesting Knudsen number range, roughly $0.15 < Kn < 1.5$, will not be accessible. The range which is accessible is expected to be done with this first arrangement.

SECTION VII
FUTURE PROGRAM

In the immediate future, the objectives are to finish debugging the present balance, complete its calibration, and to measure sphere drag in the interesting ranges accessible with the present equipment. If minor modifications give hope of covering the entire interesting sphere drag range, they will be made. Following this, the first balance is to be used to supplement the study of those design modifications which are expected to be made or seriously considered and the problems which are expected to occur in the second-generation balance. Concurrently, the design and construction of the second balance will be initiated. Those problems expected to be studied with the first balance include:

1) Use of magnetic material cores in the main field coils;

2) Use of magnetic material cores in the gradient coils;

3) Development of position sensing systems suitable for aerodynamic models.

The study of liquid-cooled coil design and construction (both main and gradient coils) should not require use of the balance. Reasonably concurrent with the design and construction of the second balance, a theoretical study of an experimental dynamic stability program utilizing an EM balance will be made. Some preliminary work of this nature has been done, but a thorough study needs to be made.

Further into the future, and assuming that the EM balance actually proves to have the potential for stability measurements which its proponents believe, it is possible to envision a group at the University of Virginia embarked on a long-term dynamic stability program in, say, the moderate supersonic speed range. It is possible to imagine other applications; e.g., low-density and hypersonic aerodynamic measurements.

ACKNOWLEDGMENT

The authors wish to acknowledge the assistance of Professor Billy Joe Gilpin, Dr. John Ging, and Mr. R. R. Humphris in various phases of the design and construction of the electronic circuits. Mr. Douglas Griffith, a graduate student in aeronautical engineering, has been responsible for adapting the existing University of Virginia wind tunnels for use with the electromagnetic balance system and for the determination of their flow properties. Finally, we are indebted to Professors A. R. Kuhlthau and John E. Scott, Jr., of the Department of Aeronautical Engineering whose many helpful suggestions, criticisms, and analyses were a constant source of stimulation.

BIBLIOGRAPHY

[1] A. W. Jenkins and H. M. Parker, "Electromagnetic support arrangement with three-dimensional control I. Theoretical," J. Appl. Phys., Supplement no. 4, vol. 30, pp. 238S-239S; 1959.

[2] H. S. Fosque and A. Miller, "Electromagnetic support arrangement with three-dimensional control II. Experimental," J. Appl. Phys., Supplement no. 4, no. 30, pp. 240S-241S; 1959.

[3] F. T. Holmes, "Axial magnetic suspensions," Rev. Sci. Instr., vol. 8, p. 444; 1937.

[4] J. W. Beams, "Ultra high speed rotation," Sci. American, vol. 204, no. 4, pp. 134-147; April, 1961.

[5] J. W. Beams, "High speed rotation," Phys. Today, vol. 12, no. 7, pp. 20-27; July, 1959.

[6] J. W. Beams, "High speed centrifuging," Revs. of Modern Phys., vol. 10, pp. 245-263; October, 1938.

[7] J. W. Beams, "Magnetic suspension balance," Phys. Rev., vol. 78, p. 471; 1950.

[8] A. R. Kuhlthau, "The investigation of low density drag phenomena utilizing laboratory techniques," Proc. Fourth U.S. Navy Symp. on Aeroballistics; November 12-14, 1957.

[9] V. A. Arkadiev, "A floating magnet," Nature, vol. 160, p. 330; 1947.

[10] I. Simon, "Forces acting on superconductors in magnetic fields," J. Appl. Phys., vol. 24, pp. 19-24; 1953.

[11] C. J. Davisson and J. W. Beams, "A new variation of the rotation by magnetisation method of measuring gyromagnetic ratios," Revs. Modern Phys., vol. 25, p. 246; 1953.

[12] M. Tournier and P. Laurenceau, "Magnetic suspension of a model in a wind tunnel," La Richerche Aeronautique, vol. 59; July-August, 1957.

[13] J. E. Chrisinger, "An Investigation of the Engineering Aspects of a Wind Tunnel Magnetic Suspension System," Master's thesis, Massachusetts Institute of Technology, Cambridge; 1959. (See also, ASTIA No. AD 221 294)

DISTRIBUTION LIST

Copy No.	
1 - 10	ASTIA Arlington Hall Station Arlington 12, Virginia ATTN: TIPCR
11 - 12	Air Force Office of Scientific Research Washington 25, D. C. ATTN: SRHM
13 - 14	Air Force Office of Scientific Research Washington 25, D. C. ATTN: SRGL
15 - 16	EOOAR Shell Building 47 Rue Cantersteen Brussels, Belgium
17	AEDC Arnold Air Force Station Tennessee ATTN: AEOIM
18	AFFTC Edwards Air Force Base California ATTN: FTOTL
19	AFMDC Holloman Air Force Base New Mexico ATTN: HDOI
20	AFMTC Patrick Air Force Base Florida ATTN: AFMTC Tech Library-MU-135
21	AFOSR (SRLTL) Holloman Air Force Base New Mexico
22 - 23	Aeronautical Systems Division Wright-Patterson Air Force Base, Ohio ATTN: WWAD

Copy No.	
24	Aeronautical Systems Division Wright-Patterson Air Force Base, Ohio ATTN: WWRMCM
25	Aeronautical Systems Division Wright-Patterson Air Force Base, Ohio ATTN: ASRNGC
26 - 27	ARL (OAR) Wright-Patterson Air Force Base, Ohio
28 - 29	Institute of Technology Library (AU) MCLI-LIB, Bldg. 125, Area B Wright-Patterson Air Force Base, Ohio
30	APGC (PGAPI) Eglin Air Force Base Florida
31 - 32	AFCRL L. G. Hanscomb Field Bedford, Massachusetts ATTN: CRRELA
33	AFSWC (SWOI) Kirtland Air Force Base Nex Mexico
34	Director BRL Aberdeen Proving Ground, Maryland ATTN: Library
35	Office of Ordnance Research Box CM Duke Station Durham, North Carolina
36	Army Rocket and Guided Missile Agency Redstone Arsenal, Alabama ATTN: Technical Library
37	Signal Corps Engineering Laboratory Fort Monmouth, New Jersey ATTN: SIGFMIEL - RPO
38	Office of the Chief of RandD Department of the Army Washington 24, D. C. ATTN: Scientific Information

Copy No.	
39	Office of Naval Research Washington 25, D. C. ATTN: Mechanics Branch
40	Office of Naval Research Washington 25, D. C. ATTN: Airbranch
41	Naval Research Laboratory Washington 25, D. C. ATTN: Documents Library
42	Naval Ordnance Laboratory White Oak, Maryland ATTN: Library
43	David Taylor Model Basin Aerodynamics Laboratory Washington 7, D. C. ATTN: Library
44	Chief, Bureau of Ordnance Department of the Navy Washington 25, D. C. ATTN: Special Projects Office, SP-2722
45	NASA 1502 H Street, N. W. Washington 25, D. C. ATTN: Document Library
46	Ames Research Center (NASA) Moffett Field, California ATTN: Technical Library
47	AFOSR Washington 25, D. C. ATTN: SRHM
48	AFOSR Washington 25, D. C. ATTN: SRGL
49	High Speed Flight Station (NASA) Edwards Air Force Base California ATTN: Technical Library

Copy No.	
50	Langley Research Center (NASA) Langley Air Force Base, Virginia ATTN: Technical Library
51	Lewis Research Center (NASA) 21000 Brookpark Road Cleveland 35, Ohio ATTN: Technical Library
52	National Bureau of Standards U. S. Department of Commerce Washington 25, D. C. ATTN: Technical Reports Section
53	Office of Technical Services U. S. Department of Commerce Washington 25, D. C. ATTN: Technical Reports Section
54	National Science Foundation 1951 Constitution Avenue, N. W. Washington 25, D. C. ATTN: Engineering Sciences Division
55	U. S. Atomic Energy Commission Technical Information Extension P. O. Box 62 Oak Ridge, Tennessee
56	U. S. Atomic Energy Commission Technical Information Service 1901 Constitution Avenue, N. W. Washington 25, D. C.
57 - 58	Southwest Research Institute 8500 Culebra Road San Antonio 6, Texas ATTN: Applied Mechanics Reviews
59	Aeronautical Engineering Review 2 East 64th Street New York 21, New York
60	Institute of Aeronautical Sciences 2 East 64th Street New York 21, New York ATTN: Library

Copy No.

61 Chairman
Canadian Joint Staff (DRB/DSIS)
2450 Massachusetts Avenue, N. W.
Washington 25, D. C.

62 Director
National Aeronautical Establishment
Ottawa, Ontario
Canada

63 University of Toronto
Institute of Aerophysics
Toronto 5, Canada
ATTN: Library

64 Training Center for Experimental Aerodynamics
Rhode-Saint-Genese (Belgique)
72, Chaussee de Waterloo, Brussels, Belgium

65 Library (Route to Dr. W. P. Jones)
Aeronautical Research Council
National Physical Laboratory
Teddington, England

66 Aeronautical Research Associates of Princeton
50 Washington Road
Princeton, New Jersey

67 Auburn University
Department of Mechanical Engineering
Auburn , Alabama

68 Brown University
Gifts and Exchanges Library
Providence 12, Rhode Island

69 University of California
Institute of Engineering Research
Low Pressures Research Project
Berkeley 4, California

70 University of California
Engineering Department
Los Angeles 24, California
ATTN: Library

71 California Institute of Technology
2800 Oak Grove Drive
Pasadena 4, California
ATTN: JPL Library

Copy No.	
72	California Institute of Technology Guggenheim Aeronautical Laboratory Pasadena 4, California ATTN: Aeronautics Library (Rte. to Prof. Liepmann)
73	Colorado State University Department of Civil Engineering Fort Collins, Colorado ATTN: Prof. J. E. Cermak, ASCE
74	Columbia University Department of Civil Engineering and Engineering Mechanics New York 27, New York ATTN: Library (Route to Prof. G. Hermann)
75	Cornell University Graduate School of Aeronautical Engineering Ithaca, New York ATTN: Library (Route to Prof. W. R. Sears)
76	Harvard University Department of Engineering Sciences Cambridge 38, Massachusetts ATTN: Library
77	John Crerar Library 86 E. Randolph Street Chicago 1, Illinois
78	The Johns Hopkins University Applied Physics Laboratory Library 8621 Georgia Avenue Silver Spring, Maryland
79	The Johns Hopkins University Department of Mechanics Baltimore 18, Maryland ATTN: Library (Rte. to Profs. Clauser and Corrsin)
80	University of Maryland Institute of Fluid Dynamics and Applied Mechanics College Park, Maryland
81	Massachusetts Institute of Technology Naval Supersonic Laboratory Cambridge 38, Massachusetts

Copy No.

82 Massachusetts Institute of Technology
Cambridge 39, Massachusetts
ATTN: Aeronautics Library

83 Massachusetts Institute of Technology
14S-226, Cambridge 39, Massachusetts
ATTN: Tech Collection

84 Massachusetts Institute of Technology
14S-226, Cambridge 39, Massachusetts
ATTN: X Collection

85 Midwest Research Institute
425 Volker Boulevard
Kansas City 10, Missouri
ATTN: Library

86 Rosemount Aeronautical Laboratories
University of Minnesota
Minneapolis, Minnesota
ATTN: Library

87 North Carolina State College
Division of Engineering Research
Raleigh, North Carolina
ATTN: Technical Library

88 Ohio State University
Department of Aeronautical Engineering
Columbus, Ohio
ATTN: Library

89 Polytechnic Institute of Brooklyn
333 Jay Street
Brooklyn 1, New York
ATTN: Library

90 Aerodynamics Laboratory
Polytechnic Institute of Brooklyn
527 Atlantic Avenue
Freeport, Long Island, New York

91 The James Forrestal Research Center
Princeton University
Princeton, New Jersey
ATTN: Library (Route to Prof. S. Bogdonoff)

Copy No.

92 Princeton University
Department of Aeronautical Engineering
Princeton, New Jersey
ATTN: Library

93 Renssealer Polytechnic Institute
Department of Aeronautical Engineering
Troy, New York
ATTN: Library

94 University of Southern California
Engineering Center (Library)
3518 University Avenue
Los Angeles 7, California

95 Stanford Research Institute
Documents Center (ATTN: Acquisitions)
Menlo Park, California

96 Stanford University
Department of Aeronautical Engineering
Stanford, California
ATTN: Library

97 Defense Research Laboratory
University of Texas
P. O. Box 8029
Austin 12, Texas

98 University of Washington
Department of Aeronautical Engineering
Seattle, Washington
ATTN: Library

99 New York University
Institute of Mathematical Sciences
New York 3, New York
ATTN: Library

100 Yale University
Department of Mechanical Engineering
New Haven 10, Connecticut
ATTN: Library (Route to Dr. P. Wegener)

101 AVCO-Everett Research Laboratory
201 Lowell Street
Wilmington, Massachusetts
ATTN: Research Library (Route to F. R. Riddell)

Copy No.

102 AVCO-Everett Research Laboratory
2385 Revere Beach Parkway
Everett 49, Massachusetts
ATTN: Technical Library (Route to Petschek)

103 Boeing Scientific Research Laboratories
P. O. Box 3981
Seattle 24, Washington
ATTN: Research Library

104 Chance-Vought Aircraft, Inc.
Dallas, Texas
ATTN: Library

105 Convair
Fort Worth Division
Fort Worth 1, Texas
ATTN: Library

106 Convair - San Diego
San Diego 12, California
ATTN: Engineering Library

107 Convair Scientific Research Laboratory
P. O. Box 950
San Diego 12, California
ATTN: Library (Rte. to Chief, Applied Research)

108 Cornell Aeronautical Laboratories, Inc.
4455 Genesse Street
Buffalo 21, New York
ATTN: Library

109 Douglas Aircraft Company, Inc.
827 Lapham Street
El Segundo, California
ATTN: Library

110 Douglas Aircraft Company, Inc.
3000 Ocean Park Boulevard
Santa Monica, California

111 Flight Sciences Laboratory
1965 Sheridan Avenue
Buffalo 23, New York
ATTN: Library (Route to Dr. J. Isenberg)

Copy No.

112 General Atomic
P. O. Box 608
San Diego 12, California
ATTN: Library

113 General Applied Sciences Laboratories, Inc.
Westbury, Long Island, New York
ATTN: Library (Rte. to Drs. Merrick, Stewart, Arnold)

114 General Electric Company
Gas Turbine Division
Cincinnati 15, Ohio
ATTN: Library (Route to Dr. Ghai)

115 General Electric Company
Research Laboratory
P. O. Box 1088
Schenectady 5, New York

116 Grumman Aircraft Engineering Corporation
Bethpage, Long Island, New York
ATTN: Library

117 Hughes Aircraft Company
Research and Development Laboratories
Culver City, California
ATTN: Library

118 Lockheed Aircraft Missile Systems Division
Palo Alto, California
ATTN: Library

119 Dr. J. Lukasiewicz
Chief von Karman Gas Dynamics Facility
ARO, Inc.
Arnold Air Force Station, Tennessee

120 The Martin Company
Denver, Colorado
ATTN: Library

121 The Martin Company
ATTN: Library
Baltimore 3, Maryland

122 Lockheed Aircraft Corporation
P. O. Box 551
Burbank, California
ATTN: Library

Copy No.

123 McDonnell Aircraft Corporation
P. O. Box 516
St. Louis 66, Missouri
ATTN: Library

124 North American Aviation, Inc.
Missile Division, ATTN: Library
12214 Lakewood Boulevard
Downey, California

125 Northrop Aircraft, Inc.
Hawthorne, California
ATTN: Library

126 Rand Corporation
1700 Main Street
Santa Monica, California

127 Republic Aviation Corporation
Farmingdale, Long Island, New York
ATTN: Library

128 United Aircraft Corporation
Research Department (Library)
400 Main Street
East Hartford 8, Connecticut

129 Unified Science Associates, Inc.
ATTN: S. Naiditch, President
926 S. Arroyo Parkway
Pasadena, California

130 Vitro Laboratories
200 Pleasant Valley Way
West Orange, New Jersey
ATTN: Library (Route to Dr. Sheer)

131 Westinghouse Electric Corporation
306 4th Avenue
Pittsburgh, Pennsylvania
ATTN: Library

132 Aeronautical Research Associates of Princeton
50 Washington Road
Princeton, New Jersey

133 MSVD Library
General Electric Company
Valley Forge Space Technology Center
King of Prussia, Pennsylvania
ATTN: L. Chasen, Library
M/F Dr. F. W. Wendt

Copy No.	
134	Dr. R. N. Zapata Gas Dynamics Group James Forrestal Research Group Princeton, New Jersey
135	A. R. Kuhlthau
136 - 137	John E. Scott, Jr.
138	Hermon M. Parker
139	Lawrence R. Quarles
140	G. Nurre
141	R. R. Humphris
142	B. J. Gilpin
143	Dr. J. Ging
144	D. B. Griffith
145	Reports Section
146 - 156	RLES Files